

Data-based predictive combustion control

Nilesh V. Kulkarni*

QSS Group, Inc., NASA Ames Research Center, Moffett Field, CA - 94035

Dawn M. McIntosh[†] and Kalmanje Krishnakumar[‡]
NASA Ames Research Center, Moffett Field, CA - 94035

George Kopasakis[§]
NASA Glenn Research Center, Cleveland, OH - 44135

An optimal predictive control approach for the suppression of thermo-acoustic instabilities in the combustor chamber is investigated. The approach uses the combustor pressure fluctuations and fuel modulation data for building internal dynamic input-output models and designing the controller. The knowledge of the physical model of the system is not required. This data-based nature of the approach is therefore useful for rapid prototyping to different geometries and new configurations without having to spend time in developing the physical models. The control approach is capable of rejecting unknown periodic disturbances to the system in an implicit manner. This capability is critical in stabilizing the pressure fluctuations in the combustor system, which is characterized by a very high noise to signal ratio. The simulation results illustrating the success of the control approach in stabilizing the pressure fluctuations are presented.

I. Introduction

Reduction of nitrous oxide (NOx) from commercial aircraft engines during take-off and landing has received significant attention in recent years. Lean combustion provides a direct way for reducing the NOx emissions and is therefore being actively researched in that context. Running the combustor lean, however, leads to thermo-acoustic instabilities which can ultimately result in stalling the engine. Several authors have looked at active control of the fuel flow rate as a means of stabilizing the combustor operation in this lean mode.¹⁻⁶ Recently an adaptive instability suppression control method has been evaluated experimentally in a successful manner.⁷ The phase of the fuel flow with respect to the combustor pressure is continuously adapted to control the pressure oscillations.

In this work we illustrate an optimal predictive control approach that uses the combustor input-output data corresponding to the fuel flow rate and combustor pressure to design a dynamic input-output feedback controller. A major advantage of this control approach lies in its capability to reject disturbances and noise in an implicit manner.⁸ One of the big problems in combustor control lies in the noise to signal ratio being very high. The dynamic input-output feedback controller is successfully able to control the combustor pressure with this high noise to signal ratio. Further having designed the controller, it does not need to be adapted to control the system if the system or the operating conditions remain unchanged. One of the concerns while running the combustor lean is to be able to control it in different operating conditions. We illustrate that the current approach can be easily used to re-compute the control gains for simulated changes in the system dynamics.

In section 2, we describe the optimal predictive control approach. We use the same model used in Ref. [7] to illustrate our control approach. Section 3 describes this model. Section 4 presents the simulation results using the optimal predictive control approach and re-computation of the control gains to handle model changes for different operating conditions.

* Scientist, M/S 269-2, AIAA Member, nilesh@email.arc.nasa.gov

[†] Computer Engineer, Code TI, M/S 269-2

[‡] Scientist and Group Lead for Adaptive Control Technologies Group, Code TI, M/S 269-2, Senior AIAA Member

[§] Controls Research Engineer, Instrumentation and Controls Division, 21000 Brookpark Road, AIAA Member

II. Control Approach

A traditional control approach involves two steps: estimating the state of the system from the given system input-output data and using this information of the estimated state to design a state feedback control. Both these steps implicitly assume the knowledge of the model of the system, which may not be available for a complex engineering system such as the engine combustor. A model derived from physical principles, even if available, can show significant differences from the working physical system, which can lead to errors in the control design. A data-based approach, on the other hand, strives to design an input-output dynamic feedback controller directly from the system input-output data. A performance-seeking controller can be designed reliably for the problem under consideration. The existence and stability of this control design depends on basic minimum requirements such as the guarantee of system observability and controllability. Phan and Juang have illustrated the use of such predictive controllers for feedback stabilization.⁸ Phan, Lim and Longman⁹ as well as Kulkarni and Phan¹⁰ have illustrated these data-based approaches and their relation to the state-feedback control design.

Every engineering system is subjected to unknown disturbances, depending on the nature of its operation. Handling these in a real environment can lead to further complexities in the control design. Phan, Juang and Eure have illustrated the applicability of the dynamic input-output data-based approaches for simultaneous feedback stabilization and disturbance rejection.¹¹ The appealing nature of this new approach lies in that it involves no new conceptual changes to the original approach presented in Ref. [9]. The only difference lies in the data length needed for the feedback control design. Recently Darling and Phan have illustrated the theoretical details of this approach for successful disturbance rejection.¹²

From a practical standpoint, this approach is very appealing for two reasons. One is that they bypass the state estimation step, which can provide big error reductions depending on the accuracy of the system modeling. The second appealing character is that it provides a performance seeking controller which leads to an overall optimal design.

The present analysis follows the theory established in Refs. [9,12]. To illustrate the optimal predictive control approach, consider a linear time invariant system

$$\mathbf{x}(k+1) = \mathbf{A}\mathbf{x}(k) + \mathbf{B}\mathbf{u}(k), \quad (1)$$

where \mathbf{A} and \mathbf{B} are the state and control transition matrices of the system. We assume that the state $\mathbf{x}(k)$ is n dimensional and the control $\mathbf{u}(k)$ is m dimensional.

We can write the future states of the system in terms of the present state and the present and future control values.

$$\mathbf{x}(k+i) = \mathbf{A}^i \mathbf{x}(k) + \mathbf{A}^{i-1} \mathbf{B} \mathbf{u}(k) + \dots + \mathbf{A} \mathbf{B} \mathbf{u}(k+i-2) + \mathbf{B} \mathbf{u}(k+i-1) \quad (2)$$

To help us with the notations, we define a supervector, $\bar{\mathbf{z}}(k)_s$ for a vector \mathbf{z} as the concatenation of its value for s time indices starting from time index k .

$$\bar{\mathbf{z}}(k)_s = \begin{bmatrix} \mathbf{z}(k) \\ \mathbf{z}(k+1) \\ \vdots \\ \mathbf{z}(k+s-1) \end{bmatrix} \quad (3)$$

Thus we can write Eq. (2) using the supervector notation as

$$\mathbf{x}(k+i) = \mathbf{A}^i \mathbf{x}(k) + \begin{bmatrix} \mathbf{A}^{i-1} \mathbf{B} & \dots & \mathbf{A} \mathbf{B} & \mathbf{B} \end{bmatrix} \bar{\mathbf{u}}(k)_i \quad (4)$$

Let the system output be given by an l dimensional vector \mathbf{y} . So the output equation can be given as

$$\mathbf{y}(k) = \mathbf{C}\mathbf{x}(k) + \mathbf{D}\mathbf{u}(k) \quad (5)$$

Translating the index by i steps, we can write,

$$\mathbf{y}(k+i) = \mathbf{C}\mathbf{x}(k+i) + \mathbf{D}\mathbf{u}(k+i) \quad (6)$$

Substituting Eq. (4) in Eq. (6), we get

$$\begin{aligned} \mathbf{y}(k+i) &= \mathbf{C}\mathbf{A}^i\mathbf{x}(k) + \mathbf{C}\begin{bmatrix} \mathbf{A}^{i-1}\mathbf{B} & \dots & \mathbf{A}\mathbf{B} & \mathbf{B} \end{bmatrix}\bar{\mathbf{u}}(k)_i + \mathbf{D}\mathbf{u}(k+i) \\ &= \mathbf{C}\mathbf{A}^i\mathbf{x}(k) + \begin{bmatrix} \mathbf{C}\mathbf{A}^{i-1}\mathbf{B} & \dots & \mathbf{C}\mathbf{A}\mathbf{B} & \mathbf{C}\mathbf{B} & \mathbf{D} \end{bmatrix}\bar{\mathbf{u}}(k)_{i+1} \end{aligned} \quad (7)$$

Eq. (7) can be translated for indices 0 through $q-1$ to get

$$\bar{\mathbf{y}}(k)_r = \begin{bmatrix} \mathbf{C} \\ \mathbf{C}\mathbf{A} \\ \vdots \\ \mathbf{C}\mathbf{A}^{r-1} \end{bmatrix} \mathbf{x}(k) + \begin{bmatrix} \mathbf{D} & \mathbf{0} & \mathbf{0} & \dots & \mathbf{0} \\ \mathbf{C}\mathbf{B} & \mathbf{D} & \mathbf{0} & \mathbf{0} & \mathbf{0} \\ \mathbf{C}\mathbf{A}\mathbf{B} & \mathbf{C}\mathbf{B} & \mathbf{D} & \mathbf{0} & \mathbf{0} \\ \vdots & \mathbf{0} & \mathbf{0} & \mathbf{0} & \mathbf{0} \\ \mathbf{C}\mathbf{A}^{r-2}\mathbf{B} & \dots & \mathbf{C}\mathbf{A}\mathbf{B} & \mathbf{C}\mathbf{B} & \mathbf{D} \end{bmatrix} \bar{\mathbf{u}}(k)_r \quad (8)$$

which can be written in a concise form as

$$\bar{\mathbf{y}}(k)_r = \mathbf{O}_r\mathbf{x}(k) + \mathbf{T}_r\bar{\mathbf{u}}(k)_r \quad (9)$$

where \mathbf{O}_r is the system observability matrix and \mathbf{T}_r is the Toeplitz matrix consisting of system Markov parameters.

Premultiplying Eq. (4) by \mathbf{O}_r gives

$$\mathbf{O}_r\mathbf{x}(k+i) = \mathbf{O}_r\mathbf{A}^i\mathbf{x}(k) + \mathbf{O}_r\begin{bmatrix} \mathbf{A}^{i-1}\mathbf{B} & \dots & \mathbf{A}\mathbf{B} & \mathbf{B} \end{bmatrix}\bar{\mathbf{u}}(k)_i \quad (10)$$

Let \mathbf{C}_i denote the controllability matrix,

$$\mathbf{C}_i = \begin{bmatrix} \mathbf{A}^{i-1}\mathbf{B} & \dots & \mathbf{A}\mathbf{B} & \mathbf{B} \end{bmatrix} \quad (11)$$

Let us assume that we have a matrix, \mathbf{I}_M , called the interaction matrix of an appropriate dimension such that

$$\begin{aligned} \mathbf{O}_r\mathbf{x}(k+i) &= \mathbf{O}_r\mathbf{A}^i\mathbf{x}(k) + \mathbf{O}_r\mathbf{C}_i\bar{\mathbf{u}}(k)_i + \mathbf{I}_M\bar{\mathbf{y}}(k)_i - \mathbf{I}_M\bar{\mathbf{y}}(k)_i \\ &= \mathbf{O}_r\mathbf{A}^i\mathbf{x}(k) + \mathbf{O}_r\mathbf{C}_i\bar{\mathbf{u}}(k)_i + \mathbf{I}_M[\mathbf{O}_r\mathbf{x}(k) + \mathbf{T}_i\bar{\mathbf{u}}(k)_i] - \mathbf{I}_M\bar{\mathbf{y}}(k)_i \\ &= (\mathbf{O}_r\mathbf{A}^i + \mathbf{I}_M\mathbf{O}_r)\mathbf{x}(k) + (\mathbf{O}_r\mathbf{C}_i + \mathbf{I}_M\mathbf{T}_i)\bar{\mathbf{u}}(k)_i - \mathbf{I}_M\bar{\mathbf{y}}(k)_i \end{aligned} \quad (12)$$

For $il > n$, we can always guarantee the existence of the matrix \mathbf{I}_M for an observable system, which satisfies the relation

$$(\mathbf{O}_r\mathbf{A}^i + \mathbf{I}_M\mathbf{O}_r) = \mathbf{0} \quad (13)$$

So we can write

$$\mathbf{O}_r \mathbf{x}(k+i) = (\mathbf{O}_r \mathbf{C}_i + \mathbf{I}_M \mathbf{T}_i) \bar{\mathbf{u}}(k)_i - \mathbf{I}_M \bar{\mathbf{y}}_i(k) \quad (14)$$

Translating the index by i and substituting the dummy variable i by q ,

$$\mathbf{O}_r \mathbf{x}(k) = (\mathbf{O}_r \mathbf{C}_q + \mathbf{I}_M \mathbf{T}_q) \bar{\mathbf{u}}(k-q)_q - \mathbf{I}_M \bar{\mathbf{y}}(k-q)_q \quad (15)$$

Substituting in Eq. (9),

$$\bar{\mathbf{y}}(k)_r = (\mathbf{O}_r \mathbf{C}_q + \mathbf{I}_M \mathbf{T}_q) \bar{\mathbf{u}}(k-q)_q - \mathbf{I}_M \bar{\mathbf{y}}(k-q)_q + \mathbf{T}_r \bar{\mathbf{u}}(k)_r \quad (16)$$

To illustrate the details, we can write Eq. (16) in an expanded form as

$$\begin{bmatrix} \mathbf{y}(k) \\ \mathbf{y}(k+1) \\ \vdots \\ \mathbf{y}(k+r-1) \end{bmatrix} = (\mathbf{O}_r \mathbf{C}_q + \mathbf{I}_M \mathbf{T}_q) \begin{bmatrix} \mathbf{u}(k-q) \\ \mathbf{u}(k-q+1) \\ \vdots \\ \mathbf{u}(k-1) \end{bmatrix} - \mathbf{I}_M \begin{bmatrix} \mathbf{y}(k-q) \\ \mathbf{y}(k-q+1) \\ \vdots \\ \mathbf{y}(k-1) \end{bmatrix} + \mathbf{T}_r \begin{bmatrix} \mathbf{u}(k) \\ \mathbf{u}(k+1) \\ \vdots \\ \mathbf{u}(k+r-1) \end{bmatrix} \quad (17)$$

Eq. (17) illustrates that the system dynamics for a linear system can be represented using the system inputs and outputs alone. Specifically the present and future outputs of the system depend on the past inputs and outputs of the system and the present and future inputs to the system. The condition for the existence of the interaction matrix depends on the size of the scalar q .

$$ql \geq n, \quad (18)$$

Let us now consider that the system represented by Eq. (1) is excited by external disturbances. So the system dynamics are now represented as

$$\mathbf{x}(k+1) = \mathbf{A}\mathbf{x}(k) + \mathbf{B}\mathbf{u}(k) + \mathbf{B}_d \mathbf{d}(k) \quad (19)$$

Ref. [12] proves that if the disturbance \mathbf{d} can be represented by a discrete number of cyclic frequencies, the system dynamics can again be represented as a dynamic input-output model.

$$\mathbf{y}(k+1) = \mathbf{A}_y \bar{\mathbf{y}}(k-q+1)_q + \mathbf{A}_{yu} \bar{\mathbf{u}}(k-q+1)_{q-1} + \mathbf{B}_y \mathbf{u}(k) \quad (20)$$

The condition on the data length q is now given equivalent to Eq. (18) as

$$ql > n + 2f + 1 \quad (21)$$

where f corresponds to the number of distinct frequencies in the external disturbance. So the disturbance information is subsumed in the dynamic input-output model and the disturbance signal does not appear explicitly in the system equations. Eq. (21) again corresponds to a one-step model. We can also obtain a r -step ahead model equivalent to Eq. (17) given by

$$\bar{\mathbf{y}}(k+1)_r = \mathbf{A}_{yr} \bar{\mathbf{y}}(k-q+1)_q + \mathbf{A}_{yur} \bar{\mathbf{u}}(k-q+1)_{q-1} + \mathbf{B}_{yr} \bar{\mathbf{u}}(k)_r \quad (22)$$

q therefore corresponds to a design variable and by choosing a large enough value, we can always satisfy Eq. (21).

Now consider minimizing a cost-to-go function in terms of system inputs and outputs

$$\begin{aligned}
V_y(k) &= \frac{1}{2} \sum_{i=1}^{r-1} \left[\mathbf{y}(k+i)^T \mathbf{Q}_y \mathbf{y}(k+i) + \mathbf{u}(k+i-1)^T \mathbf{R}_y \mathbf{u}(k+i-1) \right] \\
&= \bar{\mathbf{y}}(k+1)_r^T \bar{\mathbf{Q}}_{y_r} \bar{\mathbf{y}}(k+1)_r + \bar{\mathbf{u}}(k)_r^T \bar{\mathbf{R}}_{y_r} \bar{\mathbf{u}}(k)_r,
\end{aligned} \tag{23}$$

where the cost weighting matrices $\bar{\mathbf{Q}}_{y_r}$ and $\bar{\mathbf{R}}_{y_r}$ are given as

$$\bar{\mathbf{Q}}_{y_r} = \begin{bmatrix} \mathbf{Q}_y & \mathbf{0} & \dots & \mathbf{0} \\ \mathbf{0} & \mathbf{Q}_y & \dots & \mathbf{0} \\ \vdots & \vdots & \ddots & \mathbf{0} \\ \mathbf{0} & \mathbf{0} & \dots & \mathbf{Q}_y \end{bmatrix}, \bar{\mathbf{R}}_{y_r} = \begin{bmatrix} \mathbf{R}_y & \mathbf{0} & \dots & \mathbf{0} \\ \mathbf{0} & \mathbf{R}_y & \dots & \mathbf{0} \\ \vdots & \vdots & \ddots & \mathbf{0} \\ \mathbf{0} & \mathbf{0} & \dots & \mathbf{R}_y \end{bmatrix} \tag{24}$$

Define a vector $\bar{\mathbf{v}}(k-q)_q$ as

$$\bar{\mathbf{v}}(k-q)_q = \left[\bar{\mathbf{u}}(k-q)_q^T \quad \bar{\mathbf{y}}(k-q)_q^T \right]^T \tag{25}$$

Define matrix \mathbf{A}_{v_r} as

$$\mathbf{A}_{v_r} = \begin{bmatrix} \mathbf{A}_{y_{vr}} & \mathbf{A}_{y_r} \end{bmatrix} \tag{26}$$

Substituting Eq. (22) with the definitions given by Eqs. (25-26), in Eq. (23) we get

$$\begin{aligned}
V_y(k) &= \left[\mathbf{A}_{v_r} \bar{\mathbf{v}}(k-q)_q + \mathbf{B}_{y_r} \bar{\mathbf{u}}(k)_r \right]^T \bar{\mathbf{Q}}_{y_r} \left[\mathbf{A}_{v_r} \bar{\mathbf{v}}(k-q)_q + \mathbf{B}_{y_r} \bar{\mathbf{u}}(k)_r \right] + \bar{\mathbf{u}}(k)_r^T \bar{\mathbf{R}}_{y_r} \bar{\mathbf{u}}(k)_r \\
&= \bar{\mathbf{v}}(k-q)_q^T \mathbf{A}_{v_r}^T \bar{\mathbf{Q}}_{y_r} \mathbf{A}_{v_r} \bar{\mathbf{v}}(k-q)_q + 2 \bar{\mathbf{v}}(k-q)_q^T \mathbf{A}_{v_r}^T \bar{\mathbf{Q}}_{y_r} \mathbf{B}_{y_r} \bar{\mathbf{u}}(k)_r \\
&\quad + \bar{\mathbf{u}}(k)_r^T (\mathbf{B}_{y_r}^T \bar{\mathbf{Q}}_{y_r} \mathbf{B}_{y_r} + \bar{\mathbf{R}}_{y_r}) \bar{\mathbf{u}}(k)_r
\end{aligned} \tag{27}$$

Implementing the optimality condition,

$$\frac{\partial V_y(k)}{\partial \bar{\mathbf{u}}(k)_r} = 0 \tag{28}$$

we get

$$\begin{aligned}
2 \mathbf{A}_{v_r}^T \bar{\mathbf{Q}}_{y_r} \mathbf{B}_{y_r} \bar{\mathbf{v}}(k-q)_q + 2 (\mathbf{B}_{y_r}^T \bar{\mathbf{Q}}_{y_r} \mathbf{B}_{y_r} + \bar{\mathbf{R}}_{y_r}) \bar{\mathbf{u}}(k)_r^* &= 0 \\
\bar{\mathbf{u}}(k)_r^* &= -(\mathbf{B}_{y_r}^T \bar{\mathbf{Q}}_{y_r} \mathbf{B}_{y_r} + \bar{\mathbf{R}}_{y_r})^{-1} \mathbf{B}_{y_r}^T \bar{\mathbf{Q}}_{y_r} \mathbf{A}_{v_r} \bar{\mathbf{v}}(k-q)_q
\end{aligned} \tag{29}$$

If the optimal gain matrices are given by $\mathbf{G}_{y_1}^*$, $\mathbf{G}_{y_2}^*$, ..., $\mathbf{G}_{y_r}^*$ where,

$$\bar{\mathbf{u}}^*(k+i-1) = \mathbf{G}_{y_i}^* \bar{\mathbf{v}}(k-q)_q \tag{30}$$

then the optimal gains can be found by comparing Eqs. (29) and (30).

$$\begin{bmatrix} \mathbf{G}_{y1}^* \\ \mathbf{G}_{y2}^* \\ \vdots \\ \mathbf{G}_{yr}^* \end{bmatrix} = -(\mathbf{B}_{yr}^T \bar{\mathbf{Q}}_{yr} \mathbf{B}_{yr} + \bar{\mathbf{R}}_{yr})^{-1} \mathbf{B}_{yr}^T \bar{\mathbf{Q}}_{yr} \mathbf{A}_{vr} \quad (31)$$

In the system implementation we use the first gain matrix to compute the control

$$\mathbf{u}^*(k) = \mathbf{G}_{y1}^* \bar{\mathbf{v}}(k-q) \quad (32)$$

To compute the gains using input-output data, we extract the matrices \mathbf{A}_{vr} (\mathbf{A}_{ywr} and \mathbf{A}_{yr}), and \mathbf{B}_{yr} . The remaining matrices in Eq. (31) involve the output and control weighting matrices in the cost-to-go function that are a design choice.

Using the expanded form Eq. (22), we can write

$$\begin{bmatrix} \mathbf{y}(k) \\ \mathbf{y}(k+1) \\ \vdots \\ \mathbf{y}(k+r-1) \end{bmatrix} = \mathbf{A}_{ywr} \begin{bmatrix} \mathbf{u}(k-q) \\ \mathbf{u}(k-q+1) \\ \vdots \\ \mathbf{u}(k-1) \end{bmatrix} + \mathbf{A}_{yr} \begin{bmatrix} \mathbf{y}(k-q) \\ \mathbf{y}(k-q+1) \\ \vdots \\ \mathbf{y}(k-1) \end{bmatrix} + \mathbf{B}_{yr} \begin{bmatrix} \mathbf{u}(k) \\ \mathbf{u}(k+1) \\ \vdots \\ \mathbf{u}(k+r-1) \end{bmatrix} \quad (33)$$

This represents one data sample for Eq. (33). We can write Eq. (33) for multiple data samples as

$$\begin{bmatrix} \mathbf{y}(k)^1 & \mathbf{y}(k)^2 & \dots & \mathbf{y}(k)^p \\ \mathbf{y}(k+1)^1 & \mathbf{y}(k+1)^2 & \dots & \mathbf{y}(k+1)^p \\ \vdots & \vdots & \dots & \vdots \\ \mathbf{y}(k+r-1)^1 & \mathbf{y}(k+r-1)^2 & \dots & \mathbf{y}(k+r-1)^p \end{bmatrix} = \mathbf{A}_{ywr} \begin{bmatrix} \mathbf{u}(k-q)^1 & \mathbf{u}(k-q)^2 & \dots & \mathbf{u}(k-q)^p \\ \mathbf{u}(k-q+1)^1 & \mathbf{u}(k-q+1)^2 & \dots & \mathbf{u}(k-q+1)^p \\ \vdots & \vdots & \dots & \vdots \\ \mathbf{u}(k-1)^1 & \mathbf{u}(k-1)^2 & \dots & \mathbf{u}(k-1)^p \end{bmatrix} \quad (34)$$

$$+ \mathbf{A}_{yr} \begin{bmatrix} \mathbf{y}(k-q)^1 & \mathbf{y}(k-q)^2 & \dots & \mathbf{y}(k-q)^p \\ \mathbf{y}(k-q+1)^1 & \mathbf{y}(k-q+1)^2 & \dots & \mathbf{y}(k-q+1)^p \\ \vdots & \vdots & \dots & \vdots \\ \mathbf{y}(k-1)^1 & \mathbf{y}(k-1)^2 & \dots & \mathbf{y}(k-1)^p \end{bmatrix} + \mathbf{B}_{yr} \begin{bmatrix} \mathbf{u}(k)^1 & \mathbf{u}(k)^2 & \dots & \mathbf{u}(k)^p \\ \mathbf{u}(k+1)^1 & \mathbf{u}(k+1)^2 & \dots & \mathbf{u}(k+1)^p \\ \vdots & \vdots & \dots & \vdots \\ \mathbf{u}(k+r-1)^1 & \mathbf{u}(k+r-1)^2 & \dots & \mathbf{u}(k+r-1)^p \end{bmatrix}$$

We define the data matrices in Eq. (34) as

$$\mathbf{Y}_{\text{future}} = \begin{bmatrix} \mathbf{y}(k)^1 & \mathbf{y}(k)^2 & \dots & \mathbf{y}(k)^p \\ \mathbf{y}(k+1)^1 & \mathbf{y}(k+1)^2 & \dots & \mathbf{y}(k+1)^p \\ \vdots & \vdots & \dots & \vdots \\ \mathbf{y}(k+r-1)^1 & \mathbf{y}(k+r-1)^2 & \dots & \mathbf{y}(k+r-1)^p \end{bmatrix}, \mathbf{Y}_{\text{past}} = \begin{bmatrix} \mathbf{y}(k-q)^1 & \mathbf{y}(k-q)^2 & \dots & \mathbf{y}(k-q)^p \\ \mathbf{y}(k-q+1)^1 & \mathbf{y}(k-q+1)^2 & \dots & \mathbf{y}(k-q+1)^p \\ \vdots & \vdots & \dots & \vdots \\ \mathbf{y}(k-1)^1 & \mathbf{y}(k-1)^2 & \dots & \mathbf{y}(k-1)^p \end{bmatrix}$$

$$\mathbf{U}_{\text{future}} = \begin{bmatrix} \mathbf{u}(k-q)^1 & \mathbf{u}(k-q)^2 & \dots & \mathbf{u}(k-q)^p \\ \mathbf{u}(k-q+1)^1 & \mathbf{u}(k-q+1)^2 & \dots & \mathbf{u}(k-q+1)^p \\ \vdots & \vdots & \dots & \vdots \\ \mathbf{u}(k-1)^1 & \mathbf{u}(k-1)^2 & \dots & \mathbf{u}(k-1)^p \end{bmatrix}, \mathbf{U}_{\text{past}} = \begin{bmatrix} \mathbf{u}(k)^1 & \mathbf{u}(k)^2 & \dots & \mathbf{u}(k)^p \\ \mathbf{u}(k+1)^1 & \mathbf{u}(k+1)^2 & \dots & \mathbf{u}(k+1)^p \\ \vdots & \vdots & \dots & \vdots \\ \mathbf{u}(k+r-1)^1 & \mathbf{u}(k+r-1)^2 & \dots & \mathbf{u}(k+r-1)^p \end{bmatrix}$$

We can therefore write Eq. (33) as

$$\mathbf{Y}_{\text{future}} = \begin{bmatrix} \mathbf{A}_{\text{yur}} & \mathbf{A}_{\text{yr}} & \mathbf{B}_{\text{yr}} \end{bmatrix} \begin{bmatrix} \mathbf{U}_{\text{past}} \\ \mathbf{Y}_{\text{past}} \\ \mathbf{U}_{\text{future}} \end{bmatrix} \quad (35)$$

The system matrices, \mathbf{A}_{yur} , \mathbf{A}_{yr} , and \mathbf{B}_{yr} , can now be computed by inverting Eq. (35) as

$$\begin{bmatrix} \mathbf{A}_{\text{yur}} & \mathbf{A}_{\text{yr}} & \mathbf{B}_{\text{yr}} \end{bmatrix} = \mathbf{Y}_{\text{future}} \begin{bmatrix} \mathbf{U}_{\text{past}} \\ \mathbf{Y}_{\text{past}} \\ \mathbf{U}_{\text{future}} \end{bmatrix}^T \left\{ \begin{bmatrix} \mathbf{U}_{\text{past}} \\ \mathbf{Y}_{\text{past}} \\ \mathbf{U}_{\text{future}} \end{bmatrix} \begin{bmatrix} \mathbf{U}_{\text{past}} \\ \mathbf{Y}_{\text{past}} \\ \mathbf{U}_{\text{future}} \end{bmatrix}^T \right\}^{-1} \quad (36)$$

Substituting these matrices in Eq. (31) we can compute the control gains.

III. Combustor System Model

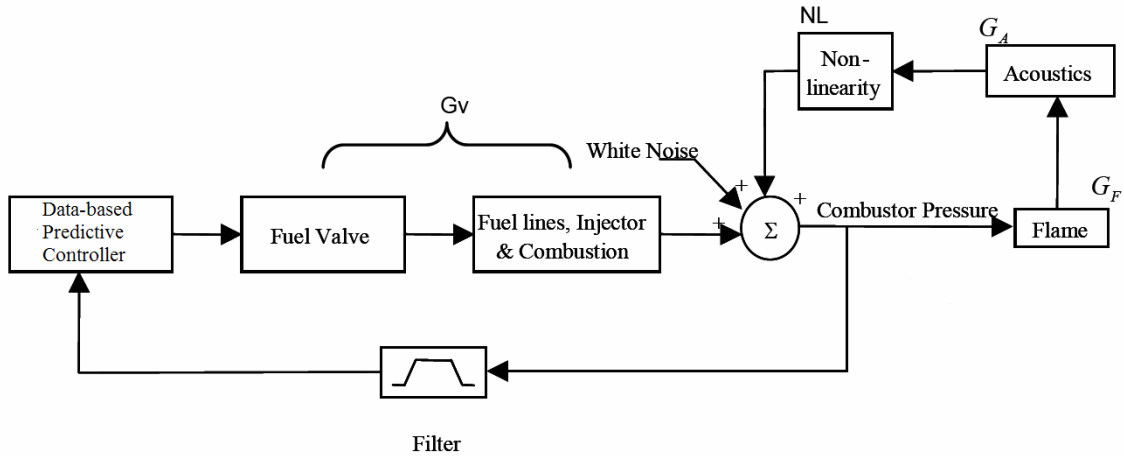


Figure 1: Combustion instability control block diagram (adapted from Ref. [7])

We use the combustor instability simulation model used in Ref. [7]. This model has been updated to model the high frequency instability typically observed in the combustor. Original work modeled low frequency instability for the system.¹³ Figure 1 illustrates the closed loop block diagram of the system with its different feedback structures. We have substituted the adaptive sliding phasor averaged control (ASPAC) algorithm that was used to control the combustor instability with the data-based predictive control algorithm described in section 2. The figure illustrates the self-sustained oscillations loop (G_F , G_A , NL) and the controller with the fuel valve actuation. In this closed loop simulation, the overall combustor pressure is expressed as the sum of the instability pressure generated by the self-excited flame and acoustics loop, and the pressure caused by the controller actuated fuel modulation. The gain and damping for the reduced-order model of this high frequency combustor simulations remain the same as the previous low frequency simulations [13]. The frequencies were changed to simulate the high frequency instability. The sampling time of 10 kHz was selected to reflect the sampling frequency of the test hardware, which defines the controlled phase resolution. Given the choices of damping and sampling time this simulation is numerically unstable (limited by the saturation nonlinearity NL), which means the open-loop response also depends on the sampling time. Numerical instability is not an undesirable feature with this simulation, as long as the results are repeatable. The purpose of the nonlinearity (NL) is to provide a soft limit for the instability. Soft limit implies that the amplitude of the instability will be limited when no forcing is applied, but also the amplitude can grow when forcing or fuel

modulation is applied. Without NL , and due to the low damping and the numerical instability, the amplitude of the simulated combustor instability will grow unbounded.

The noise level was adjusted based on the averaged wideband noise of the experimental combustor rig which produced averaged noise that was approximately 7 to 10 times higher than the instability. As before, two identical band pass filters are placed in series in the feedback path. These filters achieve two objectives: 1) filtering out the process and sensor noise; and 2) representing the dead-time phase shift in the combustion process. Normally, the time delay associated with the delivery, injection, atomization, vaporization, and burning of the fuel would be included in the deadtime phase shift of the plant. However, for convenience, this dead-time phase shift has been included in the feedback path. Note: From block diagram this is not a standard feedback control system. The filter structure and attenuation characteristics for the HF case are the same as in Ref. [19], only the band pass frequency has been updated. Based on that, the state space model of the HF band pass filter used in the simulation, with a passband frequency of 510 to 640 Hz, is given as

$$\begin{aligned}\dot{\mathbf{x}}_f &= \mathbf{A}_f \mathbf{x}_f + \mathbf{B}_f \mathbf{y}_{uf} \\ \mathbf{y}_f &= \mathbf{C}_f \mathbf{x}_f\end{aligned}\quad (37)$$

\mathbf{x}_f represents the internal state of the filter, \mathbf{y}_{uf} represents the unfiltered signal and \mathbf{y}_f represents the filtered signal.

IV. Simulation Results

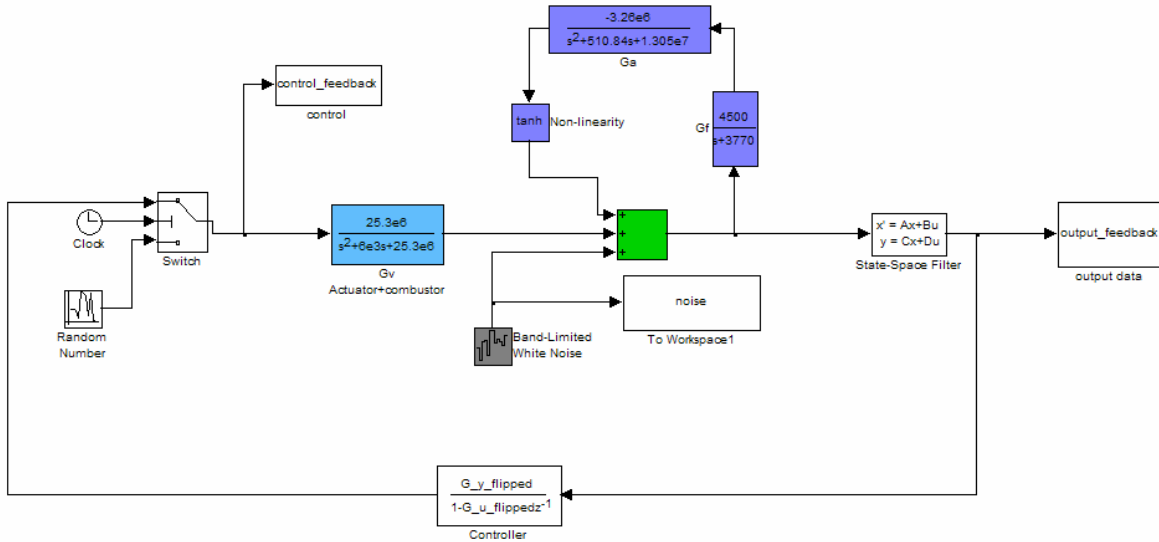


Figure 2: Combustor system input output closed-loop Simulink® architecture

The model with the feedback control loop given in figure 1. is coded using Simulink®. Figure 2 illustrates the Simulink block diagram for the control implementation. The terms $G_y_flipped$ and $G_u_flipped$ correspond to the gain matrices resolved from the optimal gain matrix $G_{y_1}^*$ as given in Eq. (32), for the output and input terms, with their coefficients flipped to match with the pole-zero notation for the discrete transfer function.

A. Open-loop Behavior

Figure 3 shows the open loop behavior of the system along with the noise characteristics used in the simulation. The open loop behavior illustrates the unstable nature of the combustion dynamics. If uncontrolled, these pressure fluctuations can easily lead to flame-out. For the open-loop simulation, the feedback loop in figure 2 is removed.

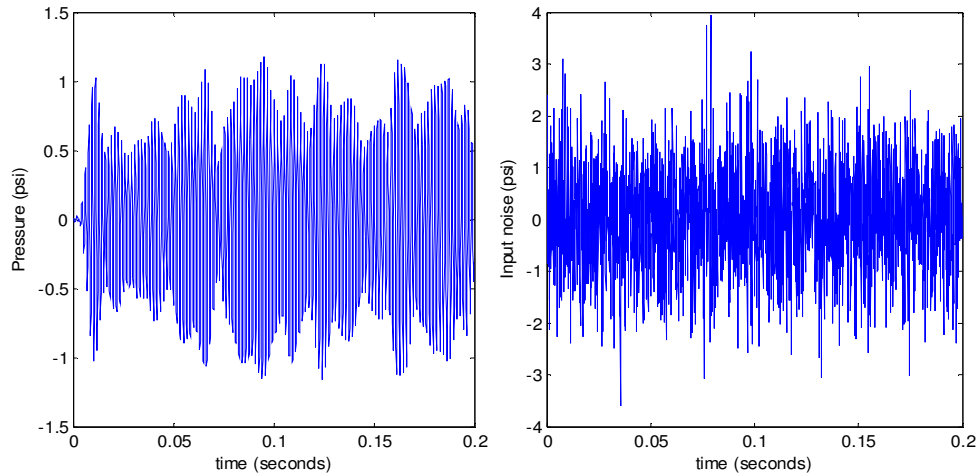


Figure 3: a) Open-loop response from the system b) Noise profile

B. Closed-loop Behavior

Figure 4 shows the closed loop response of the system using the data-based predictive control approach. For the initial 0.03 seconds, a random control profile is given to excite the system after which the designed controller takes over. Figure 5 shows the control response. The figures illustrate that the designed controller is successfully able to stabilize the pressure instability in the combustor. The average magnitude of the applied control is found to be similar to that obtained in Ref. [7]. The design variables for the controller correspond to the past data length q and the future predictive data length r . These are chosen to be 125 and 75 respectively.

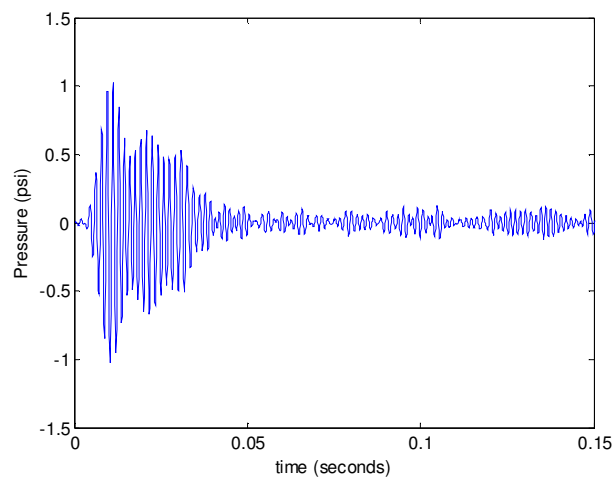


Figure 4: Closed-loop response with the data-based predictive feedback controller

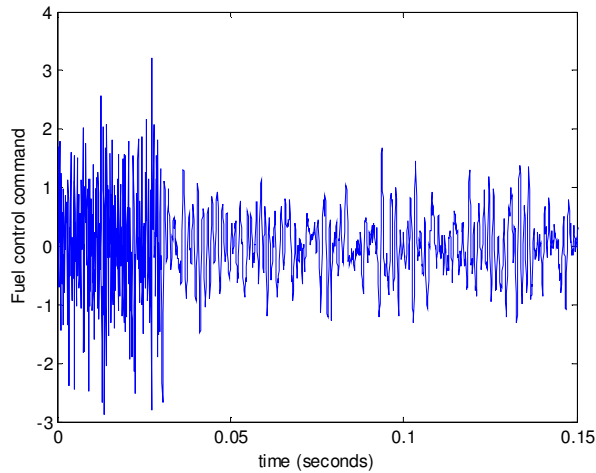


Figure 5: Fuel control command given by the data-based predictive controller

C. Re-computation of controller gains for modeling errors/changes in operating conditions:

During operation, the combustor goes through different operating conditions as the engine is taken through the entire flight envelope. The designed controller works well when designed using system input-output data that reflects the operating condition of the combustor. However it may need to be adapted to cover the entire operating envelope of the combustor. We illustrate re-tuning the controller by re-computing the controller gains while the system is in operation. The controller gains are computed in the same manner as in the closed-loop case after storing sufficient system input-output data. To illustrate differing operating conditions we change the damping ratios and the natural frequencies of the system.

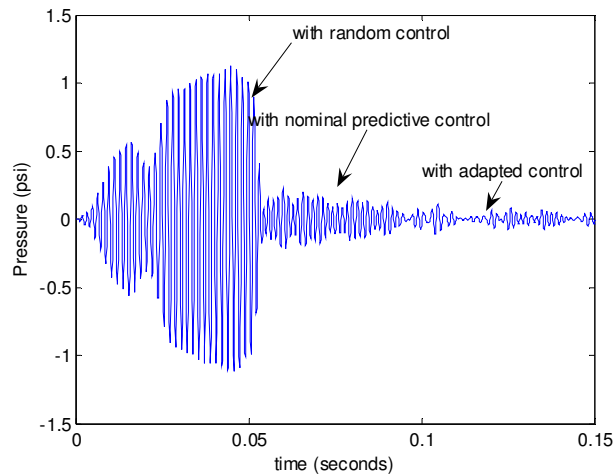


Figure 6. Pressure profile with the randomized, nominal and the adapted controller

Figure 6 illustrates the adaptation that is carried out while the system is operating. For the first 0.05 seconds, a random control profile is given to the system, then the control is given by the data-based predictive controller designed based on the data given by original model till 0.1 seconds. At $t = 0.1$ seconds, the controller re-computes the control gains after which we see the output profile based on this new adapted control profile. We see that even though the original controller tries to reduce the pressure fluctuations, the adapted controller gives a much better pressure profile and is able to suppress the fluctuations.

V. Conclusion

In this work we applied the data-based predictive control approach to control the thermo-acoustic instability in a liquid fueled combustor. The approach is successfully able to control the pressure fluctuations while being restricted by the system noise. Given combustor input-output test data, the controller can be designed in an offline setting. This controller may be valid for a particular operating condition and may not be able to stabilize the pressure fluctuations across the entire flight envelope. Similarly there could be degradations in the physical system. These reasons motivate an adaptive element in the original design. We illustrate a simple gain re-computation during system operation after collecting the system input-output data that reflects changes in the system behavior. However this approach may be realistically inappropriate based on the time involved in re-computing the control gains. Future research will investigate combining this data-based predictive control approach with various adaptive approaches that can update the control gains in a conservative yet rapid manner.

The current illustration has looked at the combustor system that has a single fuel flow actuator and a single pressure gauge sensor. Future combustor designs will include multiple fuel flow actuators for producing uniform combustion profiles in the combustor. Similarly there can be multiple pressure gauge sensors to monitor the combustion process accurately. Model based control designs would need re-modeling of the combustion process, which, can get very complex especially with multiple fuel flow actuators. However the data-based control design that we have presented can be directly applied to multiple actuator multiple sensor combustors without any modifications of the equations presented in this work. This constitutes a major advantage of this control approach.

References

- ¹McManus, K. R., Magill, J. C., and Miller, M. F., "Combustion Instability Suppression in Liquid-Fueled Combustors," *AIAA Paper* 1998-0642
- ²DeLaat, J., Breisacher, K., Saus, J., and Paxson, D., "Active Combustion Control for Aircraft Gas Turbine Engines," *AIAA Paper* 2000-3500.
- ³Johnson, C., Neumeier, Y., Lubarsky, E., Lee, J., and Zinn, B. T., "Suppression of Combustion Instabilities in a Liquid Fuel Combustor using a Fast Active Control Algorithm," *AIAA Paper* 2000-0476
- ⁴Johnson, C. E., Neumeier, Y., and Zinn, B. T., "Online Identification Approach for Adaptive Control of Combustion Instabilities," *AIAA Paper* 1999-2125.
- ⁵Boe-Shong, H., Yang, V., and Ray, A., "Robust Feedback Control of Combustion Instability with Modeling Uncertainty," *Combustion and Flame*, Vol. 120, pp 91-106, 2000.
- ⁶Cohen, J. M., Rey, N. M., Jacobson, C. A., and Anderson, T. J., "Active Control of Combustion Instability in a Liquid Fueled Low NOx Combustor," *Journal of Engineering for Gas Turbine Power*, Vol. 121, pp 281-284, 1999.
- ⁷Kopasakis, G., "High Frequency Adaptive Instability Suppression Controls in a Liquid-Fueled Combustor," 39th *Joint Propulsion Conference*, Huntsville, AL, July 2003, *AIAA Paper* 2003-4491
- ⁸Phan, M. Q., and Juang, J.-N., "Predictive Controllers for Feedback Stabilization," *Journal of Guidance, Control, and Dynamics*, Vol. 21, No. 5, Sept.-Oct., 1998, pp. 747-753.
- ⁹Phan, M. Q., Lim, R. K., and Longman, R. W., "Unifying Input-Output and State-Space Perspectives of Predictive Control," submitted to the *Journal of Vibration and Control* (preprint available at <http://www.dartmouth.edu/~mqphan>)
- ¹⁰Kulkarni, N. V., and Phan, M. Q., "Data-Based Cost-to-go Design for Optimal Control," *Proceedings of the AIAA Guidance, Navigation, and Control Conference*, Monterey, California, Aug. 2002.
- ¹¹Phan, M. Q., Juang, J.-N., and Eure, K., "Design of Predictive Controllers for Simultaneous Feedback Stabilization and Disturbance Rejection from Disturbance Corrupted Data," *Proceedings of the 137th ASA Meeting and the 2nd EAA Convention*, Berlin, Germany, March 1999.
- ¹²Darling, R. S. and Phan, M. Q., "Data-Based Design of Predictive Controllers for Periodic Disturbance Rejection," *Proceedings of the AIAA Guidance, Navigation and Control Conference*, Austin, Texas, Aug. 2003.
- ¹³Kopasakis, G., and DeLaat, J. C., "Adaptive Instability Suppression Controls in a Liquid Fueled Combustor," *Proceedings of the AIAA Joint Propulsion Conference*, Indianapolis, IN, July 2002, NASA/TM-2002-211805, AIAA-2002-4075.